Polaron energy and effective mass in a quantum well

Guo-qiang Hai, F. M. Peeters, and J. T. Devreese*
Department of Physics, University of Antwerp (UIA), Universiteitsplein 1, B-2610 Antwerp, Belgium
(Received 24 May 1990)

The polaron energy and effective mass are calculated for an electron in a quantum-well structure in the absence of a magnetic field. Interaction with interface optical-phonon modes and confined slab LO-phonon modes are incorporated in the calculation, and a comparison is made with the results in which the phonons are assumed to be three dimensional (3D). Three different confining potentials are investigated: (1) a parabolic well, (2) an infinite-barrier quantum well, and (3) the finite-barrier quantum well. A detailed study has been made of the importance of incorporating different energy levels. Our approach is able to recover the 2D and the 3D result for the case of a parabolic well and the infinite-high-barrier quantum-well model. For the quantum well with finite barrier height, we propose an approximation that leads to the correct limits.

I. INTRODUCTION

The electron–longitudinal-optical (LO) phonon interaction modifies the electronic properties of a quasi-two-dimensional (Q2D) semiconductor system, such as those found in heterostructures, quantum wells, and superlattices made of polar materials, e.g., GaAs, InAs, InSb, ... The study of the effects of the coupling of a Q2D electron system with optical phonons has received considerable attention in recent years. But in most works, the phonon modes are assumed to be the same as in the bulk material and only the electron confinement was taken into account. However, the optical phonons in a Q2D semiconductor structure are also influenced by the presence of the interfaces. Recently, the optical-phonon modes in a single heterostructure and a double heterostructure (quantum well) were studied, and the interaction of an electron with the optical phonons in these systems was established.[1–3]

The polaron effects of a Q2D electron gas interacting with optical phonons, in the presence and in the absence of a magnetic field, has been studied extensively.[4–20] In a magnetic field, the electron-phonon interaction results in the pinning of Landau levels and a shift in the cyclotron resonance frequency. Such effects resulting from interaction with 3D phonon modes have been investigated in detail.[4–11] In the absence of a magnetic field, the polaron effect induces a correction to the electron band energy and the effective band mass.[13–20] Das Sarma *et al.*[13,14] investigated the binding energy and effective mass of an electron in a $GaAs/Al_xGa_{1-x}As$ heterostructure and quantum well. In their calculation, 3D bulk LO-phonon modes of GaAs were used and the electron was confined to an infinite-barrier well. Furthermore the leading-order-term approximation was made for an electron in the lowest subband, i.e., the higher levels were not taken into account as the virtual states. Their results are valid for relative but not too narrow wells. The surface optical-phonon and slab LO-phonon modes were studied by Licari and Evrard[15] and the interaction Hamiltonian was established for a polar slab. The polaron states in such a system were studied by Licari[16] and Liang *et al.*[17] by including surface optical-phonon and slab LO-phonon modes. Comas *et al.*[18] calculated the binding energy and effective mass in a quantum well incorporating only the interaction with the confined slab LO-phonon modes. Degani and Hipólito[19,20] have incorporated interface optical-phonon and confined slab LO-phonon modes to study the polaron energy and mass in a heterostructure and a quantum well. In all the above works, it has been assumed that the electrons are confined in a quantum well with infinite high barriers.

In the present paper, we report a detailed investigation of the binding energy and the effective mass of an electron in a Q2D system induced by electron optical-phonon interaction. The interface optical-phonon and confined slab LO-phonon modes, as well as the 3D bulk LO-phonon modes, are incorporated in our calculations. Three different confining potentials will be considered: (1) parabolic well, (2) infinite-, and (3) finite-barrier square well. For the infinite-high-barrier well, all the electric levels can be included as intermediate states and, consequently, the transition of the polaronic states from 2D to 3D can be obtained as the width of the well varies from zero to infinity.

The total Hamiltonian for the coupling of an electron to the LO phonons in a Q2D system is given by (the confining potential is along the z direction)

$$H=\frac{\mathbf{p}^2}{2m_b}+V(z)+\sum_{\mathbf{q}}\hbar\omega_{\mathbf{q}}a_{\mathbf{q}}^{\dagger}a_{\mathbf{q}}+H_I\ , \tag{1}$$

where $\mathbf{p}$ is the momentum operator of the electron, m_b is the electron band mass, $V(z)$ is the confining potential, $a_{\mathbf{q}}^{\dagger}$ ($a_{\mathbf{q}}$) is the creation (annihilation) operator of a LO phonon with wave vector $\mathbf{q}$ and energy $\hbar\omega_{\mathbf{q}}$, and H_I is the electron-phonon interaction Hamiltonian, which will be specified in next section.

The energy of an electron in this system is given by

$$E_n=\frac{\hbar^2\mathbf{k}_{\parallel}^2}{2m_b}+E_{z,n}+\Delta E_n(\mathbf{k}_{\parallel})\ , \tag{2}$$

with $\mathbf{k}=(\mathbf{k}_\parallel,k_n)$ the electron wave vector, where $\mathbf{k}_\parallel$ is the component in the x-y plane, and the z component $k_z=k_n$ is quantized, $E_{z,n}$ are the discrete energy levels for the electron motion in the z direction, and $\Delta E_n(\mathbf{k}_\parallel)$ is the self-energy due to the electron-phonon interaction.

Most of the present-day quantum wells are made out of weak polar semiconductors and consequently we are allowed to use second-order perturbation theory. This gives

$$\Delta E_n(\mathbf{k}_\parallel)=-\sum_m\sum_{\mathbf{q}}\frac{|M_{nm}(\mathbf{q})|^2}{\hbar\omega_q+\hbar^2[(\mathbf{k}_\parallel-\mathbf{q}_\parallel)^2-\mathbf{k}_\parallel^2]/2m_b+E_{z,m}-E_{z,n}}\ , \tag{3}$$

where

$$M_{nm}(\mathbf{q})=\langle \mathbf{k}_\parallel-\mathbf{q}_\parallel,m;\mathbf{q}|H_I|\mathbf{k}_\parallel,n;0\rangle \tag{4}$$

is the matrix element of the electron-phonon interaction H_I, the ket $|\mathbf{k}_\parallel,m;\mathbf{q}\rangle=|\mathbf{k}_\parallel\rangle\otimes|m\rangle\otimes|\mathbf{q}\rangle$ describes a state composed of an electron in level m with momentum $\hbar\mathbf{k}_\parallel$ in the x-y plane and an optical phonon with momentum $\hbar\mathbf{q},\mathbf{q}=(\mathbf{q}_\parallel,q_z)$, and energy $\hbar\omega_q$.

The binding energy and the effective-mass correction of an electron at the bottom of the nth level can be expressed in the following form:

$$\Delta E_n=\sum_m\sum_{q_z}\frac{A}{(2\pi)^2}\times\int_0^\infty dq_\parallel\frac{q_\parallel|M_{nm}(\mathbf{q})|^2}{\hbar\omega_q+E_{z,m}-E_{z,n}+\hbar^2q_\parallel^2/2m_b}, \tag{5}$$

$$\Delta m_n^*=\sum_m\sum_{q_z}\frac{A}{(2\pi)^2}\times\int_0^\infty dq_\parallel\frac{q_\parallel^3|M_{nm}(\mathbf{q})|^2}{(\hbar\omega_q+E_{z,m}-E_{z,n}+\hbar^2q_\parallel^2/2m_b)^3}, \tag{6}$$

where A is the surface area of the 2D system.

In the rest of this paper, we will calculate the polaron binding energy and effective mass in a GaAs/$Al_xGa_{1-x}As$ quantum well. The material parameters that are used in our calculations are listed[21] in Table I. We denote the material inside the well as material 1 (GaAs) and the barrier material as material 2 ($Al_xGa_{1-x}As$) as shown in Fig. 1. The units $\hbar=\omega_{L1}=m_{b1}=1$ are used in the calculations, where m_{b1} (ω_{L1}) is the conduction-band mass (LO-phonon energy) of GaAs. The interaction Hamiltonians of an electron with different phonon modes are given in Sec. II. The binding energy and effective mass in a parabolic well are calculated in Sec. III with bulk phonon modes, and in Secs. IV and V the polaronic states in an infinite and a finite square well are calculated, respectively, with interface optical-phonon and confined slab LO-phonon modes, as well as bulk LO-phonon modes. Finally, the discussion and our conclusion are presented in Sec. VI.

II. INTERACTION HAMILTONIAN

First we give the Fröhlich interaction Hamiltonian for an electron in a Q2D system interacting with bulk LO-phonon modes:

$$H_I=\sum_{\mathbf{q}}(V_{\mathbf{q}}a_{\mathbf{q}}e^{i\mathbf{q}\cdot\mathbf{r}}+V_{\mathbf{q}}^*a_{\mathbf{q}}^\dagger e^{-i\mathbf{q}\cdot\mathbf{r}})\ , \tag{7}$$

where

$$|V_{\mathbf{q}}|^2=\frac{2\sqrt{2}\pi\alpha_1}{V}\frac{1}{q^2}$$

and α_1 is the coupling constant of the material inside the quantum well. For this case Eq. (4) reduces to

$$|M_{nm}(\mathbf{q})|^2=|V_{\mathbf{q}}|^2|G_{nm}(q_z)|^2\ , \tag{8}$$

where

$$G_{nm}(q_z)=\langle n|e^{-iq_zz}|m\rangle\ . \tag{9}$$

In doing so we ignore the effect of the quantum well on the phonon modes.

For a single quantum well, as shown in Fig. 1, the phonon modes are modified because the materials no longer extend over all space in the z direction. Actually, there are now four types of optical-phonon modes interacting with the electrons: (i) symmetric interface optical-phonon modes with frequency $\omega_{S\pm}(\mathbf{q}_\parallel)$, (ii) antisymmetric interface optical-phonon modes with frequency $\omega_{A\pm}(\mathbf{q}_\parallel)$,

TABLE I. Material parameters of GaAs and $Al_xGa_{1-x}As$ (Ref. 21).

	GaAs ($\nu=1$)	$Al_xGa_{1-x}As$ ($\nu=2$)	AlAs
α_ν	0.068	$0.068+0.058x$	0.126
$m_{b\nu}/m_{b1}$	1	$1+1.24x$	2.24
$\hbar\omega_{L\nu}$ (meV)	36.25	$36.25+3.83x+17.12x^2-5.11x^3$	50.09
$\hbar\omega_{T\nu}$ (meV)	33.29	$33.29+10.70x+0.03x^2+0.86x^3$	44.88
$\epsilon_{0\nu}$	13.18	$13.18-3.12x$	10.06
$\epsilon_{\infty\nu}$	10.89	$10.89-2.73x$	8.16

(iii) confined slab LO-phonon modes in the well with frequency ω_{L1}, and (iv) half-space LO-phonon modes in the barrier layers with frequency ω_{L2}. The electron-phonon interaction Hamiltonian now can be written in the following form:

$$H_I=\sum_j\sum_{\mathbf{q}_\parallel} e^{i\mathbf{q}_\parallel\cdot\mathbf{r}_\parallel}\Gamma_j(\mathbf{q}_\parallel,z)[a_j(\mathbf{q}_\parallel)+a_j^\dagger(-\mathbf{q}_\parallel)]\ , \tag{10}$$

where $\Gamma_j(\mathbf{q}_\parallel,z)$ is the coupling function,[1,2] which describes the coupling strength of a single electron at the position z with the jth optical-phonon mode with the dispersion relation $\omega_j(\mathbf{q}_\parallel)$. In this case, we have

$$|M_{nm}(\mathbf{q})|^2=|\langle n|\Gamma_j(\mathbf{q}_\parallel,z)|m\rangle|^2\ . \tag{11}$$

For completeness, and to avoid confusion, we give the frequency and coupling function of the different phonon modes.

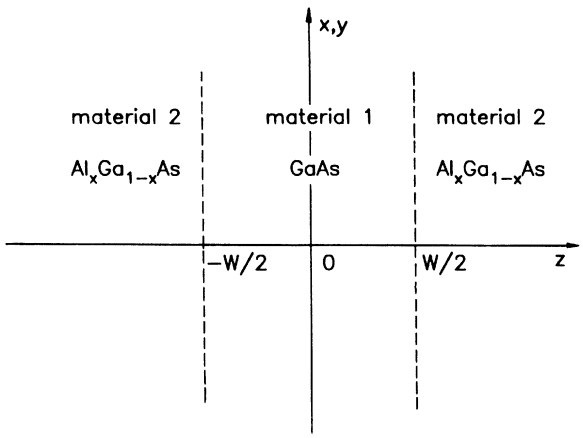

FIG. 1. Geometry of the quantum well.

A. Interface optical-phonon modes

The dispersion relation for the interface phonons is given by[2]

$$\omega_{l,\pm}(\mathbf{q}_\parallel)=\left\{\frac{1}{2(\epsilon_1^l+\epsilon_2^l)}(\epsilon_1^l(\omega_{L1}^2+\omega_{T2}^2)+\epsilon_2^l(\omega_{L2}^2+\omega_{T1}^2)\right.$$
$$\left.\pm\{[\epsilon_1^l(\omega_{L1}^2+\omega_{T2}^2)+\epsilon_2^l(\omega_{L2}^2+\omega_{T1}^2)]^2-4(\epsilon_1^l+\epsilon_2^l)(\epsilon_1^l\omega_{L1}^2\omega_{T2}^2+\epsilon_2^l\omega_{L2}^2\omega_{T1}^2)\}^2)\right\}^{1/2}\ , \tag{12}$$

where $\epsilon_1^l=\epsilon_{\infty 1}(1-\gamma_l e^{-q_\parallel W})$, $\epsilon_2^l=\epsilon_{\infty 2}(1+\gamma_l e^{-q_\parallel W})$, and $l=S,A$ refers to the symmetric (S) and antisymmetric (A) modes, respectively, $\gamma_S=1$, $\gamma_A=-1$, $\omega_{Lv}^2=\omega_{Tv}^2(\epsilon_{0v}/\epsilon_{\infty v})$, $v=1,2$, and W is the width of the quantum well. The coupling function of a single electron with the interface phonons is

$$\Gamma_{l,\pm}(\mathbf{q}_\parallel,z)=-\left[\frac{2\pi e^2\hbar}{A\omega_{l,\pm}(\mathbf{q}_\parallel)}\right]^{1/2}\frac{C_{l,\pm}}{q_\parallel}\begin{cases}e^{-q_\parallel(z-W/2)}, & z>W/2\\ f_l(q_\parallel,z), & |z|<W/2\\ \gamma_l e^{q_\parallel(z+W/2)}, & z<-W/2\ ,\end{cases} \tag{13}$$

where

$$C_{l,\pm}=\left[\frac{q_\parallel(1+\gamma_l e^{-q_\parallel W})}{2}\right]^{1/2}\left[\frac{[\omega_{T1}^2-\omega_{l,\pm}^2(\mathbf{q}_\parallel)]^2[\omega_{T2}^2-\omega_{l,\pm}^2(\mathbf{q}_\parallel)]^2}{\epsilon_1^l(\omega_{L1}^2-\omega_{T1}^2)[\omega_{T2}^2-\omega_{l,\pm}^2(\mathbf{q}_\parallel)]^2+\epsilon_2^l(\omega_{L2}^2-\omega_{T2}^2)[\omega_{T1}^2-\omega_{l,\pm}^2(\mathbf{q}_\parallel)]^2}\right]^{1/2}$$

and

$$f_S(q_\parallel,z)=\frac{\cosh(q_\parallel z)}{\cosh(q_\parallel W/2)}\ , \tag{14}$$

$$f_A(q_\parallel,z)=\frac{\sinh(q_\parallel z)}{\sinh(q_\parallel W/2)}\ . \tag{15}$$

Note that there are four interface modes whose coupling function decays exponentially as a function of the distance from the interface. As a consequence for a very thick quantum well these phonon modes will not contribute to the polaron effect because on the average the electron will be far away from the interfaces.

B. Confined slab LO-phonon modes

The coupling function of a single electron with the confined slab LO-phonon modes with frequency ω_{L1} is given by

$$\Gamma_{L1}^j(\mathbf{q}_\parallel,z)=-\left[\frac{4\pi\hbar^2\omega_{L1}\alpha_1}{AW}\left[\frac{2\hbar\omega_{L1}}{m_{b1}}\right]^{1/2}\right]^{1/2}$$
$$\times\frac{\sin[q_1^j(z+W/2)]}{[q_\parallel^2+(q_1^j)^2]^{1/2}} \tag{16}$$

for $|z|<W/2$ and is zero otherwise. The wave vector of the confined slab LO phonons is $\mathbf{q}=(\mathbf{q}_\parallel,q_1^j)$, where $q_1^j=j\pi/W$, $j=1,2,\ldots$.

C. Half-space LO-phonon modes

The coupling function of a single electron with the half-space LO-phonon modes in the barrier material with frequency ω_{L2} is given by

$$\Gamma_{L2}(\mathbf{q}_\parallel,q_z,z)=-\left[\frac{4\pi\hbar^2\omega_{L2}\alpha_2}{V_G}\left[\frac{2\hbar\omega_{L2}}{m_{b2}}\right]^{1/2}\right]^{1/2}\begin{cases}\dfrac{\sin[q_z(z-W/2)]}{(q_\parallel^2+q_z^2)^{1/2}}, & z>W/2\\ 0, & |z|<W/2\\ \dfrac{\sin[q_z(z+W/2)]}{(q_\parallel^2+q_z^2)^{1/2}}, & z<-W/2\ .\end{cases} \tag{17}$$

III. PARABOLIC QUANTUM WELL

Wide parabolic quantum wells have recently been grown[22] by tailoring the conduction-band edge of a graded $Al_xGa_{1-x}As$ semiconductor. Here we are interested in the one-electron limit of such a system. For simplicity we assume a parabolic potential extending from $z=-\infty$ to $z=+\infty$. For convenience we approximate the electron mass in this system by the conduction-band mass of GaAs. The confining potential has the following form:

$$V(z)=\tfrac{1}{2}m_{b1}\Omega^2z^2\ , \tag{18}$$

and the quantized energy levels in the z direction are given by

$$E_{z,n}=\hbar\Omega(n+\tfrac{1}{2}),\quad n=0,1,2,\ldots\ . \tag{19}$$

Considering interaction with bulk LO-phonon modes, we obtain the binding energy and the effective-mass correction for an electron in the lowest level:

$$\Delta E=\frac{\alpha_1}{\sqrt{\pi}}\int_0^\infty du\,e^{-u}\frac{\arcsin\sqrt{1-F(u)}}{\sqrt{u[1-F(u)]}}\ , \tag{20}$$

$$\Delta m^*=\frac{\alpha_1}{2\sqrt{\pi}}\int_0^\infty du\,e^{-u}\left[\frac{u}{F(u)}\right]^{1/2}\left[1-\frac{1}{1-F(u)}+\frac{\sqrt{F(u)}\arcsin\sqrt{1-F(u)}}{[1-F(u)]^{3/2}}\right]\ , \tag{21}$$

where $F(u)=(1-e^{-\Omega u})/\Omega u$.

The 3D limit is obtained by taking $\Omega\to 0$, which implies $F(u)=1$, and results into the known values

$$\Delta E=\alpha_1,\quad \Delta m^*=\frac{\alpha_1}{6}\ .$$

The 2D limit is recovered in the limit $\Omega\to\infty$, or $F(u)=0$,

$$\Delta E=\frac{\pi}{2}\alpha_1,\quad \Delta m^*=\frac{\pi}{8}\alpha_1\ .$$

In order to obtain the correct 3D limit it was essential to incorporate *all intermediate states*. To calculate the self-energy of a Q2D polaron, usually, one ignores the influences of the higher levels, i.e., only the leading term in the summation over m (i.e., $m=n$) in Eqs. (5) and (6) is taken. If this approximation is made for the parabolic quantum well, we have

$$\Delta E=\frac{\alpha_1}{\sqrt{\pi}}\int_0^\infty du\frac{e^{-u}}{\sqrt{u}}R(u)\ ,$$

$$\Delta m^*=\frac{\alpha_1}{2\sqrt{\pi}}\int_0^\infty du\,e^{-u}\left[\frac{u}{F_1(u)}\right]^{1/2}\left[1-\frac{1}{1-F_1(u)}+\frac{[F_1(u)]^{1/2}}{1-F_1(u)}R(u)\right]\ ,$$

where

$$R(u)=\begin{cases}\dfrac{\ln\{[F_1(u)-1]^{1/2}+[F_1(u)]^{1/2}\}}{[F_1(u)-1]^{1/2}}, & u<1/\Omega\\ \dfrac{\arcsin[1-F_1(u)]^{1/2}}{[1-F_1(u)]^{1/2}}, & u>1/\Omega\end{cases}$$

with $F_1(u)=1/\Omega u$. Still, the ideal 2D result can be obtained for $\Omega\to\infty$, but the limit $\Omega\to 0$ gives $\Delta E\sim\Omega^{1/2}\ln\Omega\to 0$ and $\Delta m^*\sim\Omega^{1/2}\to 0$.

The binding energy and effective mass have been calculated numerically as a function of the inverse of the confinement frequency ω_{L1}/Ω. Thus increasing ω_{L1}/Ω implies increasing the width of the parabolic quantum well. We refer our results with respect to the ideal two-dimensional (I2D) result

$$\Delta E_r=\Delta E/\Delta E^{\mathrm{I2D}}\ , \tag{22}$$

$$\Delta m_r^*=\Delta m^*/(\Delta m^*)^{\mathrm{I2D}}\ , \tag{23}$$

where $\Delta E^{I2D}=\pi\alpha_1/2$, and $(\Delta m^*)^{I2D}=\pi\alpha_1/8$.

The full [Eqs. (20) and (21)] and leading-term-approximation results for the binding energy and effective mass of a polaron in a parabolic quantum well are shown in Figs. 2(a) and 2(b), respectively. Both results start from the ideal 2D result at $\omega_{L1}/\Omega=0$ and decrease monotonically with increasing ω_{L1}/Ω, or decreasing confinement. Only the result where all intermediate states are taken into account approaches the 3D result when $\Omega\to 0$. Note that the leading-term approximation can only be justified when $\Omega/\omega_{L1}>20$ for the energy and $\Omega/\omega_{L1}>5$ for the mass.

IV. INFINITE-BARRIER QUANTUM WELL

In this case, the confining potential is given by

$$V(z)=\begin{cases}0, & |z|<W/2\\ \infty, & |z|>W/2\end{cases} \tag{24}$$

and the energy levels and the wave functions can be obtained analytically:

$$E_{z,n}=\frac{\hbar^2\pi^2}{2m_{b1}W^2}n^2, \quad n=1,2,3,\ldots \tag{25}$$

and

$$\psi_n(z)=\begin{cases}\sqrt{2/W}\sin[(z+W/2)n\pi/W], & |z|\le W/2\\ 0, & |z|>W/2\ .\end{cases} \tag{26}$$

The importance of this model is that all the levels in the Q2D system can be incorporated in our calculations and we will be able to investigate when the leading-term approximation is correct. Intuitively, one expects that the leading-term approximation is valid when the distance between two levels is larger than the relevant excitation energy ($E_{z,2}-E_{z,1}\gg\hbar\omega_{LO}$). This study is relevant for the next section, where we study the finite-barrier quantum-well system. In such a system it is practically impossible to incorporate all levels.

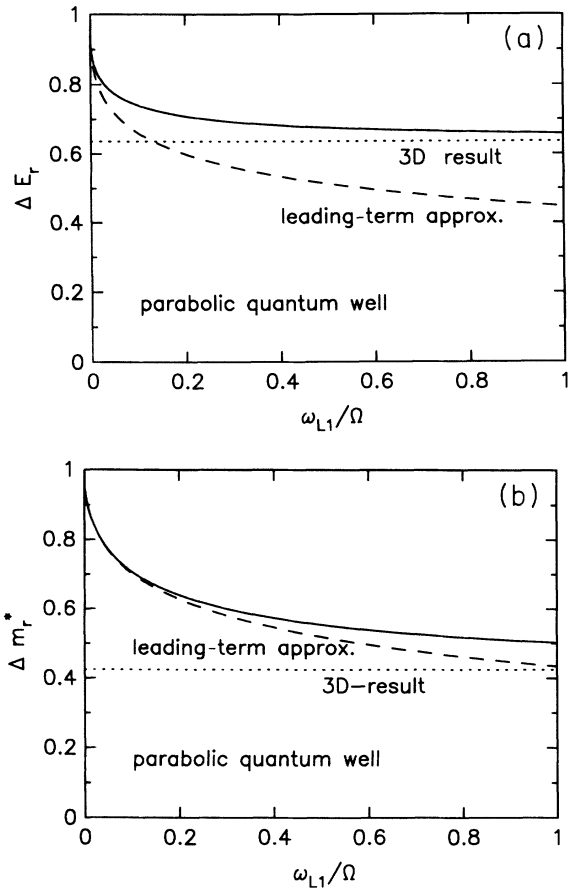

FIG. 2. (a) Polaron binding energy and (b) effective mass as a function of the inverse parabolic well confinement frequency ω_{L1}/Ω. Solid and dashed curves correspond to the full (all intermediate states) and the leading term approximate results, respectively. Dotted line indicates the 3D limit.

A. 3D bulk LO-phonon modes

The binding energy and effective mass with 3D LO-phonon modes can be obtained from Eqs. (5), (6), (8), (9), (25), and (26), for an electron in the lowest subband,

$$\Delta E=\frac{\sqrt{2}\alpha_1}{\pi}\sum_{m=1}^{\infty}\int_0^{\infty}dq_z|G_{1m}(q_z)|^2\frac{\ln\{q_z^2/2[1+E_z(m^2-1)]\}}{q_z^2-2[1+E_z(m^2-1)]}\ , \tag{27}$$

$$\Delta m^*=\frac{\alpha_1}{\sqrt{2}\pi}\sum_{m=1}^{\infty}\int_0^{\infty}dq_z\int_0^{\infty}dx\frac{x|G_{1m}(q_z)|^2}{(q_z^2+x)[1+E_z(m^2-1)+x/2]^3}\ , \tag{28}$$

where $E_z=\hbar^2\pi^2/2m_{b1}W^2$ and

$$|G_{nm}(q_z)|^2=\left[\frac{8nm\pi^2q_zW}{[(m-n)^2\pi^2-(q_zW)^2][(m+n)^2\pi^2-(q_zW)^2]}\right]^2\begin{cases}\sin^2(q_zW/2), & m+n=\text{even}\\ \cos^2(q_zW/2), & m+n=\text{odd}\ .\end{cases}$$

The sum $\sum_{m=1}^{\infty}$ is over all intermediate confining states $\psi_m(z)$.

Both the binding energy and the effective mass in an infinite-barrier quantum well with 3D LO-phonon modes have been computed as a function of the well width according to Eqs. (27) and (28), and are shown in Figs. 3(a) and (b), respectively. The leading-term-approximation results (dashed curves) are also plotted and are represented by the dashed lines. Both results start from the 2D values of GaAs at the well width $W=0$ and decrease with increasing W. We ob-

serve that the leading-term approximation is only valid for $W<60$ Å for the energy and $W<180$ Å for the effective mass. Note also that the 3D result is obtained for $W\approx 300$ Å for the energy correction and $W\approx 600$ Å for the effective mass.

B. Interface and confined slab phonon modes

The binding energy and effective-mass correction for an electron in the lowest subband interacting with interface phonons can be obtained from Eqs. (5), (6), (11), (13), (25) and (26),

$$\Delta E_{l,\pm}=\frac{\alpha_1}{\sqrt{2}}\sum_{m=1}^{\infty}\int_0^{\infty}dq_{\parallel}\frac{(1+\gamma_l e^{-q_{\parallel}W})B_{l,\pm}(q_{\parallel})}{(1/\epsilon_{\infty 1}-1/\epsilon_{01})\omega_{l,\pm}(q_{\parallel})}\frac{|G^l_{1m}(q_{\parallel})|^2 g_l^2(q_{\parallel})}{\hbar\omega_{l,\pm}(q_{\parallel})+E_z(m^2-1)+\hbar^2 q_{\parallel}^2/2m_b}\ , \tag{29}$$

$$\Delta m^*_{l,\pm}=\frac{\alpha_1}{\sqrt{2}}\sum_{m=1}^{\infty}\int_0^{\infty}dq_{\parallel}\frac{(1+\gamma_l e^{-q_{\parallel}W})B_{l,\pm}(q_{\parallel})}{(1/\epsilon_{\infty 1}-1/\epsilon_{01})\omega_{l,\pm}(q_{\parallel})}\frac{q_{\parallel}^2|G^l_{1m}(q_{\parallel})|^2 g_l^2(q_{\parallel})}{[\hbar\omega_{l,\pm}(q_{\parallel})+E_z(m^2-1)+\hbar^2 q_{\parallel}^2/2m_b]^3}\ , \tag{30}$$

where

$$B_{l,\pm}(q_{\parallel})=\frac{[\omega_{T1}^2-\omega_{l,\pm}(q_{\parallel})]^2[\omega_{T2}^2-\omega_{l,\pm}(q_{\parallel})]^2}{\epsilon_1^l(\omega_{L1}^2-\omega_{T1}^2)[\omega_{T2}^2-\omega_{l,\pm}^2(q_{\parallel})]^2+\epsilon_2^l(\omega_{L2}^2-\omega_{T2}^2)[\omega_{T1}^2-\omega_{l,\pm}^2(q_{\parallel})]^2}\ ,$$

$$|G^S_{nm}(q_{\parallel})|^2=\begin{cases}\left[\dfrac{8nm\pi^2 q_{\parallel}W}{[(q_{\parallel}W)^2+(m-n)^2\pi^2][(q_{\parallel}W)^2+(m+n)^2\pi^2]}\right]^2, & m+n=\text{even}\\ 0, & m+n=\text{odd}\ ,\end{cases}$$

$$|G^A_{nm}(q_{\parallel})|^2=\begin{cases}0, & m+n=\text{even}\\ \left[\dfrac{8nm\pi^2 q_{\parallel}W}{[(q_{\parallel}W)^2+(m-n)^2\pi^2][q_{\parallel}W)^2+(m+n)^2\pi^2]}\right], & m+n=\text{odd}\ ,\end{cases}$$

and

$$g_S(q_{\parallel})=\tanh(q_{\parallel}W/2),\ g_A(q_{\parallel})=\coth(q_{\parallel}W/2)\ .$$

The binding energy and effective-mass correction due to the interaction with the slab LO phonons can be obtained from Eqs. (5), (6), (11), (16), (25), and (26), for an electron in the lowest subband,

$$\Delta E_{\text{slab}}=2\sqrt{2}W\alpha_1\sum_{m=1}^{\infty}\sum_{j=1}^{j_{\max}}|G^j_{1m}|^2\frac{\ln\{(j\pi)^2/2W^2[1+E_z(m^2-1)]\}}{(j\pi^2-2W^2[1+E_z(m^2-1)]}\ , \tag{31}$$

$$\Delta m^*_{\text{slab}}=2\sqrt{2}W\alpha_1\sum_{m=1}^{\infty}\sum_{j=1}^{j_{\max}}\int_0^{\infty}dq_{\parallel}\frac{q_{\parallel}^3|G^j_{1m}|^2}{[(j\pi)^2+(q_{\parallel}W)^2][1+E_z(m^2-1)+q_{\parallel}^2/2]^3}\ , \tag{32}$$

where

$$|G^j_{nm}|^2=\begin{cases}0, & j+m+n=\text{even}\\ \left[\dfrac{8mnj/\pi}{[j^2-(m-n)^2][j^2-(n+m)^2]}\right]^2, & j+m+n=\text{odd}\ .\end{cases}$$

In this infinite-barrier quantum-well model, the electron wave function does not extend into the barrier material and there is no contribution from the half-space LO phonons.

The polaron correction to the binding energy and effective mass in a GaAs/AlAs quantum well with infinite barrier wells is shown in Figs. 3(a) and 3(b), respectively. The separate contribution due to interface optical-phonons and the confined slab LO-phonons are also plotted together with the leading term approximation (dashed curves). The interface phonon contributions to both the binding energy and the effective mass starts from the 2D values of AlAs, $\Delta E=\alpha_2\pi/2$ and $\Delta m^*=\alpha_2\pi/8$, at $W=0$ and decrease with increasing width. While, the confined slab LO-phonon contribution starts from zero and increases as the well width increases. The total polaron correction, i.e., interface plus slab modes, is a monotonously decreasing function of the well width. The polaron binding energy correction is for $W>240$Å within 10% of the 3D value of GaAs (dotted line in Fig. 3(a)) and for $W>150$Å within 10% of the 3D phonon mode result. Note that the leading term approximation un-

derestimates the binding energy with more than 10% when $W > 70$Å. For the polaron mass correction we find that the 3D GaAs result is reached within 10% for $W > 290$Å, while the 3D-phonon mode result differs within less than 10% when $W > 20$Å. The leading term approximation deviates with more than 10% from the full calculation when $W > 190$Å. We observe that for a quantum well with infinitely high barriers the interface phonon modes play an important role in very narrow quantum wells and in this limit the bulk phonon modes are no longer adequate to describe the Q2D problem. On the other hand, the polaron effect depends mainly on the slab phonon modes for wide-quantum-well systems and, in this case, they approach the results from the bulk phonon modes. For the leading-term approximation, the more narrow the quantum well, the larger the distance between the energy levels, and the better this approximation.

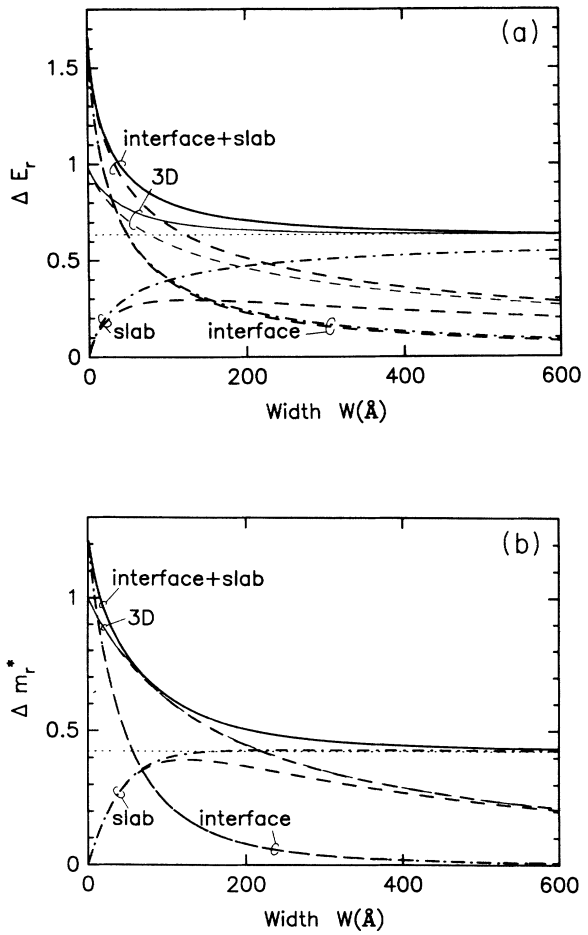

FIG. 3. (a) Polaron binding energy and (b) effective mass as a function of the well width in an infinite barrier quantum well with interface, confined slab, and 3D phonon modes. Solid and dashed curves correspond to the full (all intermediate states) and the leading term approximate results, respectively. Dot-dashed curves represent the contributions from interface and slab modes with the full calculation. Dotted line indicates the 3D limit.

V. THE FINITE-BARRIER QUANTUM WELL

In this section we will investigate the polaron states for a finite-barrier quantum-well model. Although this is a realistic model for a single quantum well, it is quite difficult to incorporate all the higher levels because the intermediate states are not known analytically. Therefore we will limit ourselves to the leading-term-approximation result. As an example, we take the GaAs/$Al_xGa_{1-x}As$ quantum-well system. Two assumptions will be made concerning the $Al_xGa_{1-x}As$ material: (i) only the interaction with one effective LO-phonon mode will be considered, and (ii) the electron is assumed to be in the Γ band. Assumption (i) follows the construction presented in Ref. 23. Assumption (ii) is exact when $x < 0.4$. For $x > 0.4$ the lowest conduction band is the X band, but for the moment we will not discuss this extra complication. In this model, the confining potential can be expressed in the following form:

$$V(z)=\begin{cases}0, & |z| < W/2 \\ V_0, & |z| > W/2\end{cases}, \tag{33}$$

where $V_0 = 0.6\times(1.155x + 0.37x^2)$ eV for a GaAs/$Al_xGa_{1-x}As$ quantum well. The wave function in the z direction for an electron in the lowest subband is given by

$$\psi_1(z)=\begin{cases}B_0\cos(kz), & |z| \le W/2 \\ B_0\cos(kW/2)e^{-k_1(|z|-W/2)}, & |z| > W/2\end{cases}, \tag{34}$$

where $k=(2m_{b1}E_1)^{1/2}/\hbar$, $k_1=[2m_{b2}(V_0-E_1)]^{1/2}/\hbar$, and E_1 is determined by the following equation:

$$\tan\left[\frac{W}{2}\frac{(2m_{b1}E_1)^{1/2}}{\hbar}\right]=\left[\frac{m_{b1}(V_0-E_1)}{m_{b2}E_1}\right]^{1/2}; \tag{35}$$

the normalization constant B_0 is given by

$$B_0=\left[\frac{2k}{kW+\sin(kW)+2k\cos^2(kW/2)/k_1}\right]^{1/2}.$$

A. 3D bulk LO-phonon modes

The binding energy and effective mass can be obtained from Eqs. (5), (6), (8), (9), and (34):

$$\Delta E=\frac{\sqrt{2}\alpha_1}{\pi}\int_0^\infty dq_z|G_{11}(q_z)|^2\frac{\ln(q_z^2/2)}{q_z^2-2} \tag{36}$$

and

$$\Delta m^*=\frac{\sqrt{2}\alpha_1}{\pi}\int_0^\infty dq_z\frac{|G_{11}(q_z)|^2}{2-q_z^2}\times\left[1+\frac{2q_z^2}{2-q_z^2}+\frac{4q_z^2\ln(q_z^2/2)}{(2-q_z^2)^2}\right], \tag{37}$$

where

$$G_{11}(q_z)=B_0^2\left[2\cos^2(kW/2)\frac{2k_1\cos(q_zW/2)-q_z\sin(q_zW/2)}{4k_1^2+q_z^2}+\frac{\sin[(2k-q_z)W/2]}{2(2k-q_z)}+\frac{\sin[(2k+q_z)W/2]}{2(2k+q_z)}+\frac{\sin(q_zW/2)}{q_z}\right].$$

We have computed the binding energy and the effective mass in a GaAs/$Al_xGa_{1-x}As$ quantum well for different Al concentration x and as a function of the well width. The results are shown in Figs. 4(a) and 4(b), respectively, for $x=0.3$ (dashed curves) and $x=1$ (solid curves). For broad wells the results are similar to what we have found with the leading-term approximation in the infinite-barrier wells. From the knowledge of the preceding section we know that our results are only realistic for narrow wells. When the well is very narrow, the results for the binding energy and the effective mass in Fig. 4 are quite different from those of an infinite-barrier well and they approach zero at $W=0$. The reason is that the more narrow the quantum well, the higher the lowest level, and at $W\to 0$ the level energy will equal the barrier height V_0. Then the continuum energy states outside the well will play an important role and the leading-term approximation is no longer valid. The leading-term approximation, in this case, is valid only for not too wide and not too narrow finite-barrier quantum wells.

B. Interface and confined slab phonon modes

For symmetric interface phonon modes, we have, from Eqs. (5), (6), (11), (13), (14), and (34),

$$\Delta E_{S,\pm}=\frac{\alpha_1}{\sqrt{2}}\int_0^\infty dq_\parallel\frac{(1+e^{-q_\parallel W})B_{S,\pm}(q_\parallel)}{(1/\epsilon_{\infty 1}-1/\epsilon_{01})\omega_{S,\pm}(q_\parallel)}\frac{|G^S(q_\parallel)|^2}{[\hbar\omega_{S,\pm}(q_\parallel)+\hbar^2q_\parallel^2/2m_b]},\tag{38}$$

$$\Delta m^*_{S,\pm}=\frac{\alpha_1}{\sqrt{2}}\int_0^\infty dq_\parallel\frac{(1+e^{-q_\parallel W})B_{S,\pm}(q_\parallel)}{(1/\epsilon_{\infty 1}-1/\epsilon_{01})\omega_{S,\pm}(q_\parallel)}\frac{q_\parallel^2|G^S(q_\parallel)|^2}{[\hbar\omega_{S,\pm}(q_\parallel)+\hbar^2q_\parallel^2/2m_b]^3},\tag{39}$$

where

$$G^S(q_\parallel)=B_0^2\left[\frac{2\cos^2(kW/2)}{2k_1+q_\parallel}+\left[\frac{1}{q_\parallel}+\frac{q_\parallel\cos(kW)}{4k^2+q_\parallel^2}\right]\tanh(q_\parallel W/2)+\frac{2k\sin(kW)}{4k^2+q_\parallel^2}\right].$$

For antisymmetric interface phonon modes, we have $\Delta E_{A\pm}=0$ and $\Delta m^*_{A\pm}=0$ from Eqs. (5), (6), (11), (13), (15), and (34).

For confined slab LO-phonon modes. we have, from Eqs. (5), (6), (11), (16), and (34),

$$\Delta E_{\rm slab}=2\sqrt{2}W\alpha_1\sum_{j=1}^{j_{\max}}|G_{11}^j|^2\frac{\ln[(j\pi)^2/2W^2]}{(j\pi)^2-2W^2},\tag{40}$$

$$\Delta m^*_{\rm slab}=2\sqrt{2}W\alpha_1\sum_{j=1}^{j_{\max}}\frac{|G_{11}^j|^2}{2W^2-(j\pi)^2}\left[1+\frac{2(j\pi)^2}{2W^2-(j\pi)^2}+\frac{4(j\pi)^2W^2\ln[(j\pi)^2/2W^2]}{[2W^2-(j\pi)^2]^2}\right],\tag{41}$$

$$G_{11}^j=\begin{cases}0, & j=\text{even}\\ B_0^2\left[\dfrac{W}{j\pi}+\dfrac{j\pi W\cos(kW)}{(j\pi)^2-4(kW)^2}\right], & j=\text{odd}.\end{cases}$$

For half-space LO-phonon modes, we have $\Delta E_{\rm barrier}=0$ and $\Delta m^*_{\rm barrier}=0$ from Eqs. (5), (6), (11), (17), and (36).

The total polaron binding energy is $\Delta E=\Delta E_{S+}+\Delta E_{S-}+\Delta E_{A+}+\Delta E_{A-}+\Delta E_{\rm slab}+\Delta E_{\rm barrier}$ and the correction to the effective mass is $\Delta m^*=\Delta m^*_{S+}+\Delta m^*_{S-}+\Delta m^*_{A+}+\Delta m^*_{A-}+\Delta m^*_{\rm slab}+\Delta m^*_{\rm barrier}$. The results are shown in Figs. 4(a) and 4(b) and we find that, for the wide well, both the contributions from interface and slab phonons have a similar behavior as compared to the leading-term approximation for the infinite-barrier-well results as shown in Fig. 3, which gives $\Delta E\sim\ln W/W\to 0$, $\Delta m^*\sim 1/W\to 0$ when $W\to\infty$. For very narrow wells the leading-term approximation is not valid for the finite-barrier case and the interface phonon contributions vanish at zero well width. Note also that the barrier height strongly influences both the binding energy and the effective mass in a narrow well in which the polaron effect mainly depends on the interface phonons.

When we compare the results from the different phonon modes (3D modes versus slab and interface modes) for the polaron corrections to the effective mass and the binding energy we find again that the interface and slab phonons give a polaron contribution that is larger than that for interaction with 3D phonons for the same well width. The peaks in Δm^* and ΔE versus W occur nearly

at the same W for the different phonon modes. In Δm^* the peak occurs at $W=10$ Å for $x=1$ and at $W=30$ Å for $x=0.3$. For ΔE the peak occurs at $W=9$ Å for $x=1$ and at $W=28$ Å for $x=0.3$. Note also that for lower barrier heights (thus smaller x) the differences between the results with 3D phonons and with interface and slab phonons are smaller. From the results of this section, we conclude that the finite-barrier quantum-well model with the leading-term approximation is only adequate to study the polaron states in wells that are not too narrow (after the peak position) and not too wide. Therefore, it is not possible to obtain the correct $W\rightarrow 0$ and $W\rightarrow\infty$ limits from this approximation.

VI. DISCUSSION AND CONCLUSION

We have investigated the polaron binding energy and effective mass in a Q2D GaAs/$Al_xGa_{1-x}As$ quantum-well system. With the infinite-barrier quantum-well model, our result shows that both the effective mass and the binding energy for interaction with 3D phonons are able to give the correct 2D and 3D limits of GaAs as the well width varies from zero to infinity. In the case of interaction with interface and slab phonons, the 2D values of the barrier AlAs are obtained in the $W\rightarrow 0$ limit while the 3D result of GaAs is found for $W\rightarrow\infty$. At the same time, the calculation of the leading-term approximation shows that this approximation is good for narrow wells. For the finite-barrier-well model, we were only able to obtain results within the leading-term approximation and we find that the leading-term approximation is not adequate for very narrow finite-barrier quantum wells and very wide quantum wells. It is obvious that for very narrow quantum wells the interaction between the electron and half-space LO phonons of the barrier material is important. When the well width becomes zero, the 3D result of the barrier material should be obtained. Within the leading-term approximation, however, there is no contribution to the binding energy and effective mass due to the LO phonons outside the well. To take into account the contribution from the LO phonons of the barrier material, we approximate their contribution by

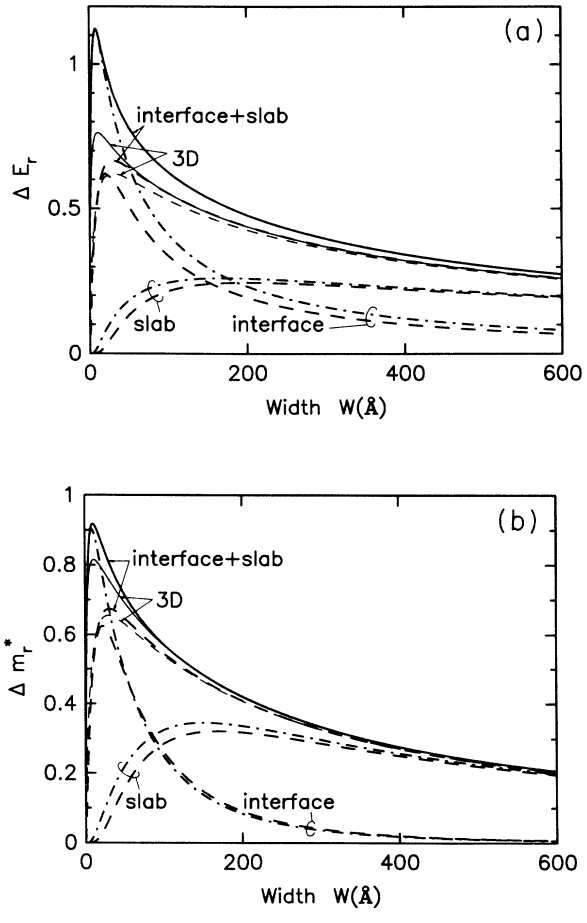

FIG. 4. (a) Polaron binding energy and (b) effective mass in a GaAs/$Al_xGa_{1-x}As$ quantum well as a function of the well width with interface, confined slab, and 3D phonon modes. Solid and dashed curves correspond to $x=1$ and 0.3, respectively. Dot-dashed curves represent the contributions from interface and slab modes for $x=1$.

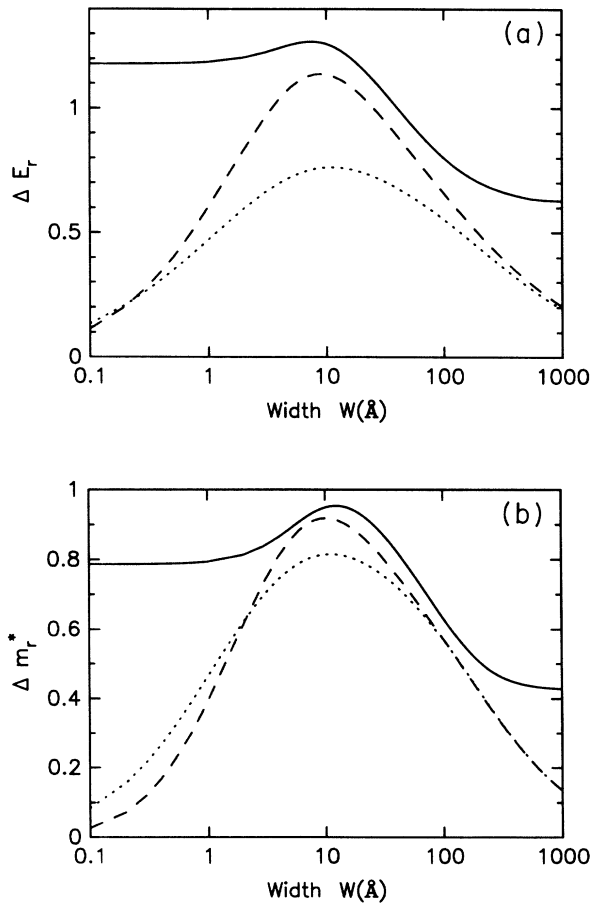

FIG. 5. (a) Polaron binding energy and (b) effective mass in a GaAs/$Al_xGa_{1-x}As$ quantum well, for $x=1$, as a function of the well width. Solid curves correspond to our new model results. Dashed and dotted curves correspond to the leading term approximation results with interface and slab modes and 3D phonon modes, respectively.

$$\Delta E_{\text{barrier}} = (1-P)\alpha_2 , \tag{42}$$

$$\Delta m^*_{\text{barrier}} = (1-P)\frac{\alpha_2}{6} , \tag{43}$$

where $P = \int_{-W/2}^{W/2} |\psi_1(z)|^2 dz$ is the probability to find the electron inside the quantum well.

For wide quantum wells the leading-term approximation leads to a zero result instead of the 3D polaron results of GaAs. The reason is that the separation between the energy levels becomes much smaller than the LO-phonon energy, i.e., $E_2 - E_1 \ll \hbar\omega_{\text{LO}}$, and higher intermediate states are relevant. In order to correct for this, we propose the following approximation to the polaron correction in the quantum well:

$$\Delta E_{\text{QW}} = P\,\Delta E_{\text{IQW}} , \tag{44}$$

$$\Delta m^*_{\text{QW}} = P\,\Delta m^*_{\text{IQW}} , \tag{45}$$

where ΔE_{IQW} (Δm^*_{IQW}) is the binding energy (polaron mass correction) for a polaron in an infinite-barrier quantum well as obtained in Sec. IV. The total polaron correction in this approximation is now given by $\Delta E = \Delta E_{\text{barrier}} + \Delta E_{\text{QW}}$ and $\Delta m^* = \Delta m^*_{\text{barrier}} + \Delta m^*_{\text{QW}}$. This result is shown by the solid curve in Figs. 5(a) and 5(b) for $x = 1$ together with the leading-term approximation of Sec. V. The result for 3D phonons (dotted curve) and slab and interface modes (dashed curve) are shown. A logarithmic scale is used for the width in order to accentuate the $W \to 0$ and $W \to \infty$ limits. Note that this approximation is able to recover the correct 3D limits for $W \to 0$ ($Al_xGa_{1-x}As$ result) and $W \to \infty$ (GaAs result), respectively.

In conclusion, the polaron binding energy and effective mass were studied in the present paper for a parabolic well, infinite-, and finite-barrier square wells. The interface optical-phonon and confined slab LO-phonon modes were incorporated in the calculations. The calculations with 3D phonon modes were also done and a comparison of the results with the different phonon modes was made. For the infinite-barrier quantum wells, either the parabolic or the square well, the transitions from the 2D to the 3D limit were correctly obtained and it was shown that the often-used leading-term approximation is only valid for narrow quantum wells. For the finite-barrier wells, the leading-term-approximation results were obtained. We also find that 3D phonon modes are quite adequate to study Q2D polaron effects in a quantum well with low barrier height. But this approximation is only valid for intermediate values of the quantum-well width. In the limit $W \to 0$ and $W \to \infty$, the polaron correction reduces to zero within the leading-term approximation. Therefore, we have proposed a new approximation, based on intuitive arguments, which is able to obtain the correct $W \to 0$ and $W \to \infty$ limits for both the finite- and infinite-high-barrier quantum wells.

ACKNOWLEDGMENTS

One of us (F.M.P.) is supported by the Belgian National Science Foundation. G. H. wishes to thank the University of Antwerp (UIA) for support.

*Also at University of Antwerp (RUCA), B-2020 Antwerp, Belgium, and The Technical University of Eindhoven, Eindhoven, The Netherlands.

[1]L. Wendler, Phys. Status Solidi B **129**, 513 (1985).
[2]L. Wendler and R. Pechstedt, Phys. Status Solidi B **141**, 129 (1987).
[3]N. Mori and T. Ando, Phys. Rev. B **40**, 6175 (1989).
[4]S. Das, Sarma and A. Madhukar, Phys. Rev. B **22**, 2823 (1980).
[5]L. Lassnig and W. Zawadzki, Surf. Sci. **142**, 388 (1984).
[6]F. M. Peeters and J. T. Devreese, Phys. Rev. B **31**, 3689 (1985).
[7]X. Wu, F. M. Peeters, and J. T. Devreese, Phys. Rev. B **34**, 8800 (1986).
[8]D. Larsen, Phys. Rev. B **35**, 4427 (1987).
[9]X. Wu, F. M. Peeters, and J. T. Devreese, Phys. Rev. B **40**, 4090 (1989).
[10]F. M. Peeters, X. Wu, and J. T. Devreese, Solid State Commun. **65**, 1505 (1988).
[11]D. M. Larsen, Phys. Rev. B **30**, 4595 (1984).
[12]X. Wu, F. M. Peeters, and J. T. Devreese, Phys. Rev. B **31**, 3420 (1985).
[13]S. Das Sarma, Phys. Rev. B **27**, 2590 (1983).
[14]S. Das Sarma and M. Stopa, Phys. Rev. B **36**, 9595 (1987).
[15]J. J. Licari and R. Evrard, Phys. Rev. B **15**, 2254 (1977).
[16]J. J. Licari, Solid State Commun. **29**, 625 (1979).
[17]X. X. Liang, S. W. Gu, and D. L. Lin, Phys. Rev. B **34**, 2807 (1986).
[18]F. Comas, C. Trallero-Giner, and R. Riera, Phys. Rev. B **39**, 5907 (1989).
[19]M. H. Degani and O. Hipólito, Phys. Rev. B **35**, 7717 (1987).
[20]M. H. Degani and O. Hipólito, Superlattices and Microstructures **5**, 141 (1989).
[21]S. Adachi, J. Appl. Phys. **58**, R1 (1985).
[22]E. G. Gwinn, R. M. Westervelt, P. F. Hopkins, A. J. Rimberg, M. Sundaram, and A. C. Gossard, Phys. Rev. B **39**, 6260 (1989); A. J. Rimberg and R. M. Westervelt, Phys. Rev. B **40**, 3970 (1989); T. Sajoto, J. Jo, L. Engel, M. Santo, and M. Shayegan, Phys. Rev. B **39**, 10 464 (1989).
[23]T. Ando, A. B. Fowler, and F. Stern, Rev. Mod. Phys. **54**, 437 (1982).